Design, Molecular Docking, Synthesis, Preliminary In Silico ADME Studies, and Anti-inflammatory Evaluation of New Oxazole Derivatives

Mahmood Amer[1*], Monther Faisal Mahdi[2], Ayad Kareem Khan[2], Ayad Mohammed Rasheed Raauf[2]

[1*]Department of Immunization, Al Zaafaraniya Hospital, Rasafa Health Directorate, MOH. E-mail: mahmoodamer22@gmail.com

[2]Department of Pharmaceutical Chemistry, College of Pharmacy, Mustansiriyah University, Baghdad, Iraq.

Abstract

Synthesis of lead compounds is a necessity. Challenges are evolving day by day, Inflammation is a must to consider. A series of new oxazole derivatives were synthesized and evaluated for their anti-inflammatory effects. The new derivatives were synthesized by incorporating an oxazole moiety into a furan molecule as a starting molecule to form furan oxazole amine as an intermediate. In silico evaluation methods were done before synthesis through molecular docking via genetic optimization for ligand docking (GOLD) Suite software with COX-2 enzyme.

The prepared compounds showed good activity against standard compounds, theoretically and experimentally.

Compounds (P1 and P2) were tested in an in vitro study to inhibit the activity of cyclooxygenase enzyme (COX-2) using RAW 264.7 cell line, and compared to anti-inflammatory drugs (SC560 and Celecoxib).

All results of biological experiments were similar to the results of *In silico* evaluation. These new derivatives were successfully synthesized in good quantities and the chemical composition was confirmed by FTIR, ^{1}HNMR, and ^{13}CNMR spectroscopy.

The pharmacokinetic and physicochemical properties of the synthesized compounds were also measured using the Swiss ADME server. The results showed that all the prepared compounds had high oral bioavailability and good absorption in the digestive system and that some compounds had low toxicity.

Keywords: Drug Design, New Oxazole Derivatives, Inhibitors, Schiff Base, Aldehydes, *In silico* Prediction, Molecular Docking, Inflammation.

DOI: 10.47750/pnr.2022.13.S07.033

INTRODUCTION

Infections and the immune system have always been linked to inflammation. However, more recent researches indicate that inflammation may be a telling sign of a far wider spectrum of disorders. The fundamental process for tissue restoration following injury is inflammation. [1-3] Cancer-related inflammation affects many aspects of malignancy, including the proliferation and survival of malignant cells, angiogenesis, tumor metastasis, and tumor response to chemotherapeutic drugs and hormones. Moreover, epidemiologic studies and meta-analyses have shown that prolonged use of non-steroid anti-inflammatory (NSAID) drugs reduces the risk of several solid tumors including lung and breast cancer. [4, 5, & 6] In general, it has become clear that the effects of NSAIDs in the prevention of gastrointestinal tract cancers, breast cancer, and lung cancer are astonishing facts. [7 & 8]

Bifunctional oxidoreductase enzymes that convert arachidonic acid to prostaglandin are named cyclooxygenase (COX) which are classified into COX-1 and COX-2. It has been extensively studied how prostaglandins, specifically PGE2, and cyclooxygenases, notably COX-2, contribute to the inflammation associated with cancer. However, COX-1 expression rises in many human malignancies, and laboratory models show that it plays a pathogenetic function. When it comes to the pathophysiology of cancer, COX-1 and COX-2 isoforms appear to work in concert, particularly throughout the carcinogenesis process. [9]

In the majority of tissues, COX-1 is expressed by default. The inducible isoform of COX, COX-2, on the other hand, is what causes increased prostanoid production in response to inflammatory stimuli and growth factors during inflammation and numerous clinical diseases, including cancer. [10] Both COX-1 and COX-2 enzymes are homodimers comprising three domains: an epidermal growth factor domain, a membrane-binding domain, and an active-site cavity (ASC) for catalysis. [11] Both isoforms are internal membrane-bound enzymes with almost identical amino acid sequences in the active site that possess four amphipathic helices with hydrophobic interactions near the

ASC. The hydrophobic "pocket" of COX-2 is located at the deep end of the ASC, whereas the ASC entrance is surrounded by the amino acid residues arginine (Arg)120, Tyr355, and glutamic acid (Glu)524, and is known as the "lobby" center. [9]

The substrate-binding site is located from Arg120 to near Tyr385. COX-2 has a larger binding cavity (17%) compared with COX-1. The exchange of Val at position 523 with a sterically hindered Ile residue causes an additional sub-pocket so that structurally bulkier inhibitors can fit into the ASC and no longer inhibit COX-1. Arg513 can interact with polar moieties within the ASC of COX-2. Simultaneously, the swing-out of Val434 might increase further access to the active site compared with that of COX-1 with the Ile434 residue. Slight structural differences in the active site modulate the selectivity profile of the compounds. [9]

Bearing a 5-membered, doubly unsaturated ring with an oxygen atom in position 1 and a nitrogen atom in position 3, the 1,3-oxazoles nucleus has a wide range of pharmacological activities, specifically when considering inflammation. Furthermore, the conjugation of oxazole moiety into Schiff base derivatives boosted their anti-inflammatory activity. [12] **Figure 1** presents such compounds. In addition, embracing both oxazole and Schiff base moieties using furan rings empowers their effect. [13,14, &15]

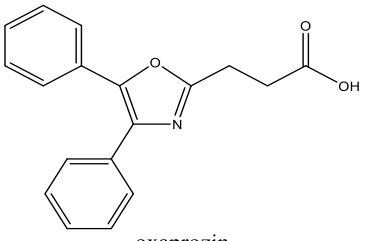

oxaprozin

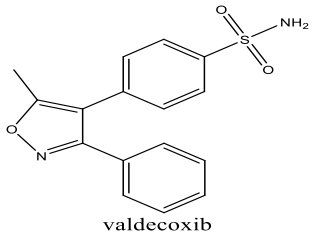

valdecoxib

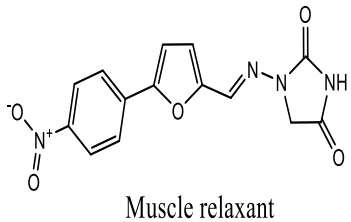

Muscle relaxant

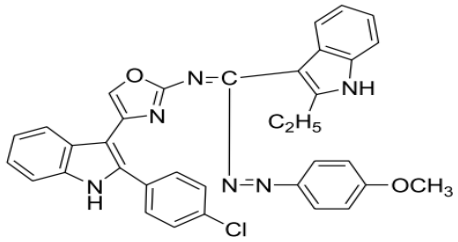

Figure 1: Furan, oxazole, and Schiff base containing compounds with promising anti-inflammatory activity.

The direction of the present study firstly by predicting the target of a receptor for biological activity by in-silico cheminformatics software and docking studies, thereafter the chemical synthesis of these derivatives by incorporating a group of oxazole core, a heterocyclic ring system, in the ketone group of 2-acetyl furan and connecting them through a Schiff base moiety into different aromatic ring cores using two different aldehydes and evaluate their activities using cell line technology that measures fluorescence which will be utilized to examine the compounds' anti-inflammatory effect.

RESULTS AND DISCUSSION

1. Docking analysis

GOLD (Genetic Optimization for Ligand Docking) is a genetic algorithm for docking flexible ligands into protein binding sites [16]. GOLD Suite has demonstrated perfect performance for pose prediction and excellent results for virtual screening. [17]

Successful docking was done using GOLD Suite software for all newly synthesized compounds. The newly synthesized compounds exhibited excellent anti-inflammatory activity. The docking results predict the binding energies and selectivity of the ligands for COX enzymes by studying the contact interactions among the active binding sites of the proteins, and designed compounds. The PLP fitness of the docked compounds on COX enzymes was found 72.82, for P1 and 85.97, for P2 as shown in **tables (2-1 and 2-2)**.

Docking analysis for COX enzymes indicated that ARG 120, TYR 385, TYR 355, VAL 116, TRP 387, SER 353, ALA 516, VAL 523, MET 522, and TRP 387 amino acid residues of COX 2 active site listed in the **table (2-2**) interact with our final ligands library (P1 and P2) via hydrogen bonding and short contact interactions and show comparable activity with COX2. **Figures (2 to 4)** illustrate binding interactions of Celecoxib, compounds P1, and compound P2.

Table (2-1): The Binding Energies for target compounds (P1 and P2) compared to standards, docked in the COX-2 enzyme.

Compound	Docking score	Compound	Docking score

	on COX enzymes		on COX-2 enzyme
P1	72.82	Celecoxib	84.85
P2	85.97	Diclofenac	71.26
	Ibuprofen		51.84

Table (2-2): The Binding Energies for target compounds (P1, P2) docked in the COX-2 enzyme.

Compounds	Amino Acids Included in H-bonding	Binding Energy (PLP Fitness)	Amino Acids Included in short contact Interactions
P1	ARG 120 (2)*	72.82	TYR 385, TYR 355, VAL 116, ARG 120, VAL 523, MET 522, TRP 387 (3)*
P2	TYR 355	85.97	TRP 387, SER 353 (2)*, VAL 523 (2)*, ALA 516
CELECOXIB	GLN 192, LEU 352, SER 353	84.85	SER 353 (3)*, VAL 349, TYR 385 (2)*, LEU 353, PHE 518

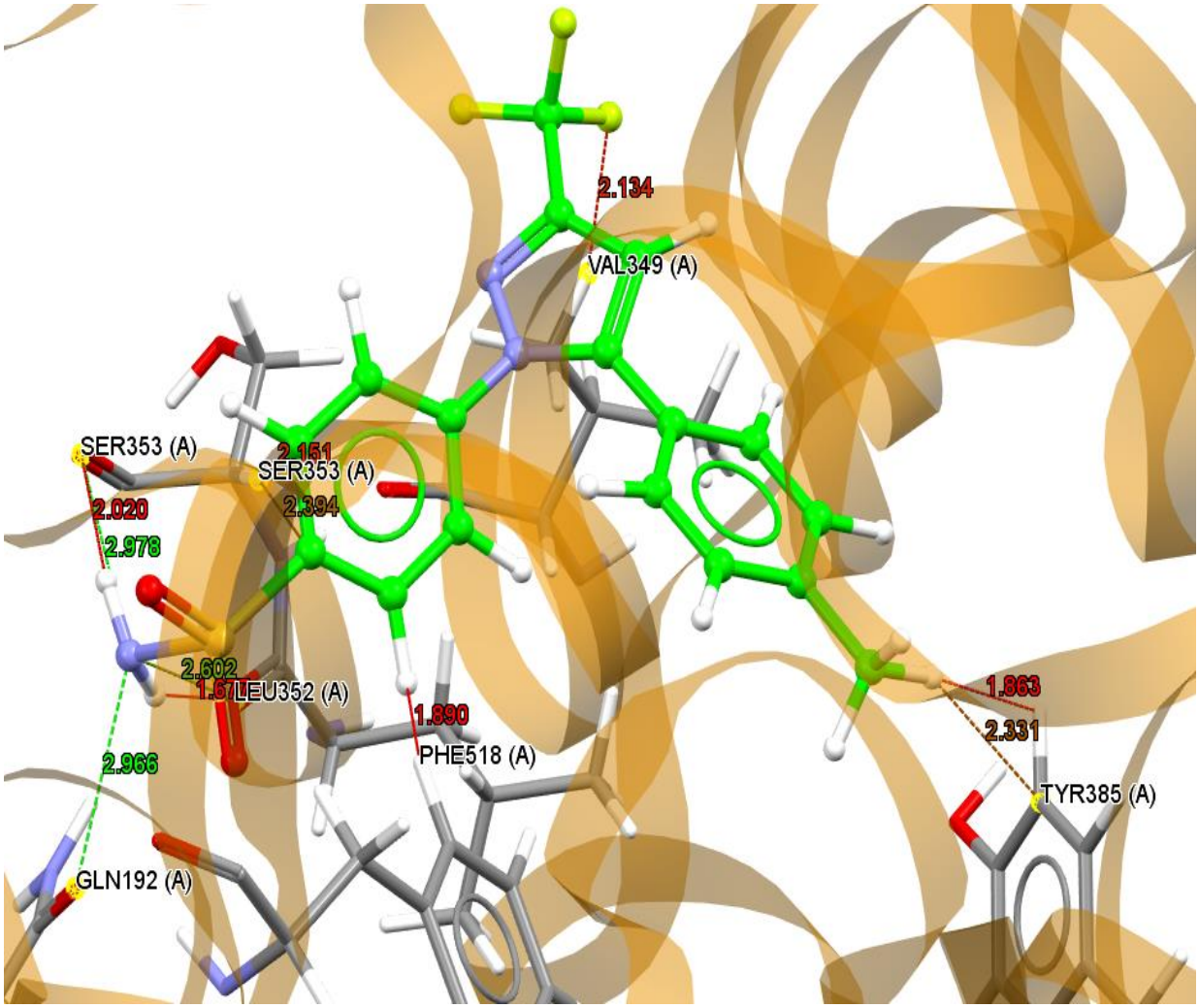

Figure 2: H-bond and short contact interaction profile for Celecoxib binding with COX-2 receptor (PDB code: 1PXX). The interaction between Celecoxib and amino acid residues by H-bond [GLN 192, LEU 352, and SER 353]. [Celecoxib: ball and stick style, while amino acids in capped sticks].

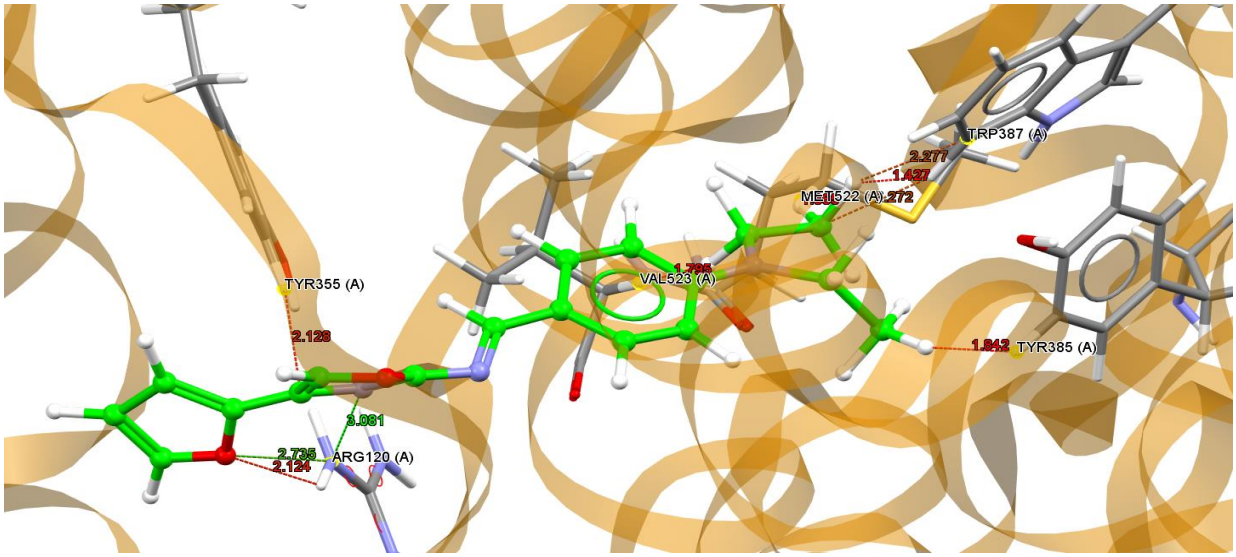

Figure 3: H-bond and short contact interaction profile for compound (P1) binding with COX-2 receptor (PDB code: 1PXX). The interaction between compound (P1) and amino acid residues by H-bond [ARG 120]. [P1: ball and stick style, while amino acids in capped sticks].

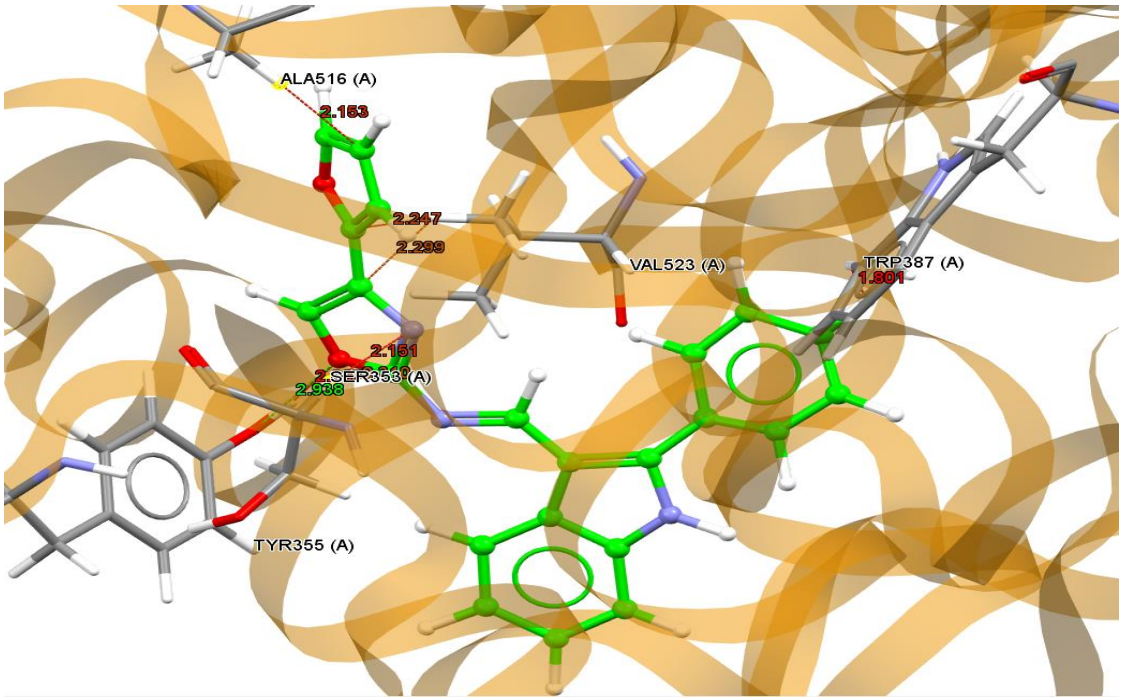

Figure 4: H-bond and short contact interaction profile for compound (P2) binding with COX-2 receptor (PDB code: 1PXX). The interaction between compound (P2) and amino acid residues by H-bond [TYR 355]. [P2: ball and stick style, while amino acids in capped sticks].

The dose response for all compounds was plotted over log-transformed concentrations. IC_{50} values were determined using nonlinear regression analysis (Prism Pad 8.1) and the results represent triplicate data.

2. In vitro study of anti-inflammatory activity of P1 and P2

In vitro study for inhibition of cyclooxygenase (COX) activity enzyme by two synthesized compounds (P1 and P2) using RAW 264.7 cell line as compared with anti-Inflammatory controls (SC560 and Celecoxib). Results were (6.3 µM and 3.48 µM) for P1 and P2 respectively. As shown in **figures (5, 6, and 7)**.

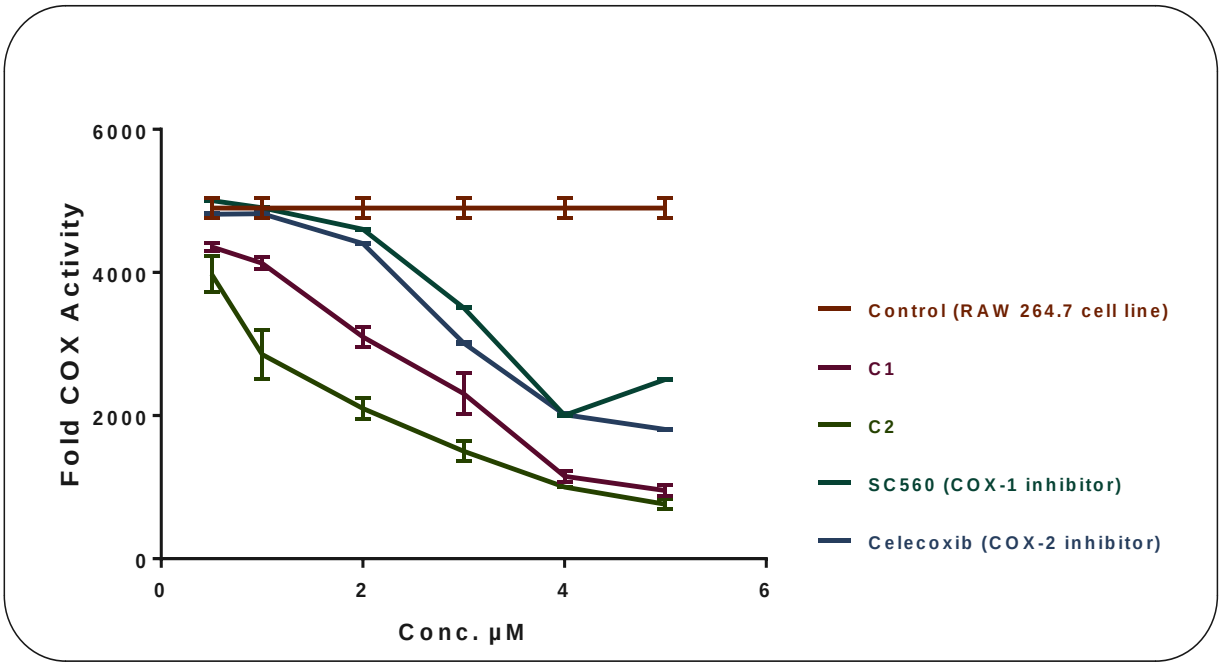

Figure 5: Measurement of the inhibitory effect of COX activity by compounds (P1 and P2) compounds. COX activity was decreased with 1 – 5µM of compounds (P1 and P2) more than the inhibitory activity of SC560 and Celecoxib (COX-1 and COX-2 inhibitors respectively as a positive control) at the same concentration.

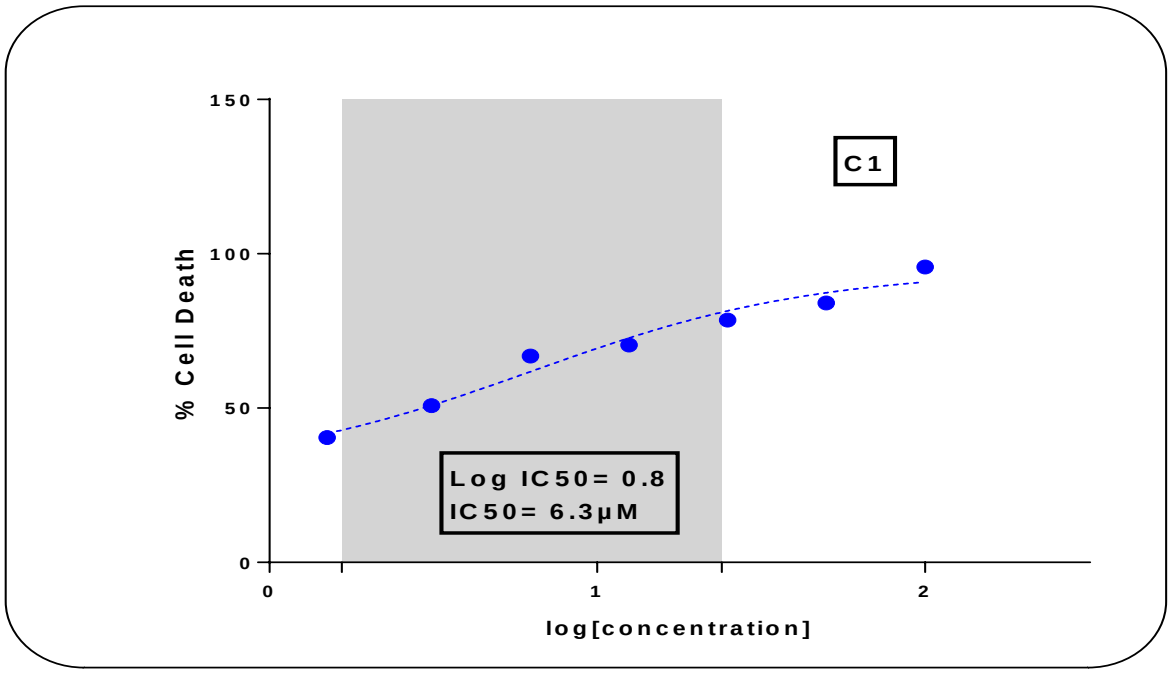

Figure 6: Dose-response curve of IC_{50} for compound **(P1)**. RAW 264.7 cells were treated for 72h with 1.56, 3.12, 6.25, 12.5, 25, 50, and 100 µM dose ranges of (**P1)**. The dose-response for compound (**P1)** was plotted over log transformed compound **P1** concentrations. IC_{50} values were determined using nonlinear regression analysis (Prism Pad 8.1). Results represent triplicate data.

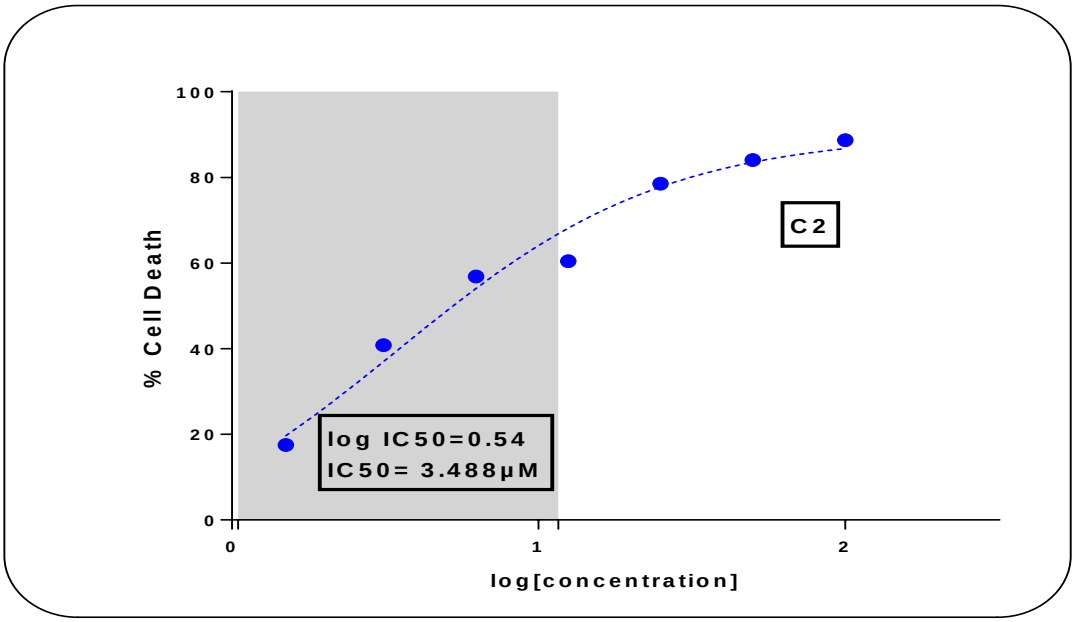

Figure 7: Dose-response curve of IC_{50} for compound (**P2**). RAW 264.7 cells were treated for 72h with 1.56, 3.12, 6.25, 12.5, 25, 50, and 100 µM dose ranges of (**P2**). The dose-response for compound (**P2**) was plotted over log transformed compound (**P2**) concentrations. IC_{50} values were determined using nonlinear regression analysis (Prism Pad 8.1). Results represent triplicate data.

Figure 8 demonstrates COX enzyme activity, where axis Y represents fluorescence data of COX activity for compounds (**P1** and **P2**) divided by fluorescence data of COX activity at zero time. While axis X representing logarithmic concentrations of 0.008 nM, 0.012 nM, 0.016 nM, and 0.02 nM from compounds (**P1**) and (**P2**) as compared with the activity of 0.02 nM SC560 (COX-1 inhibitor as a positive control) and 0.02 nM Celecoxib (COX-2 inhibitor as a positive control).

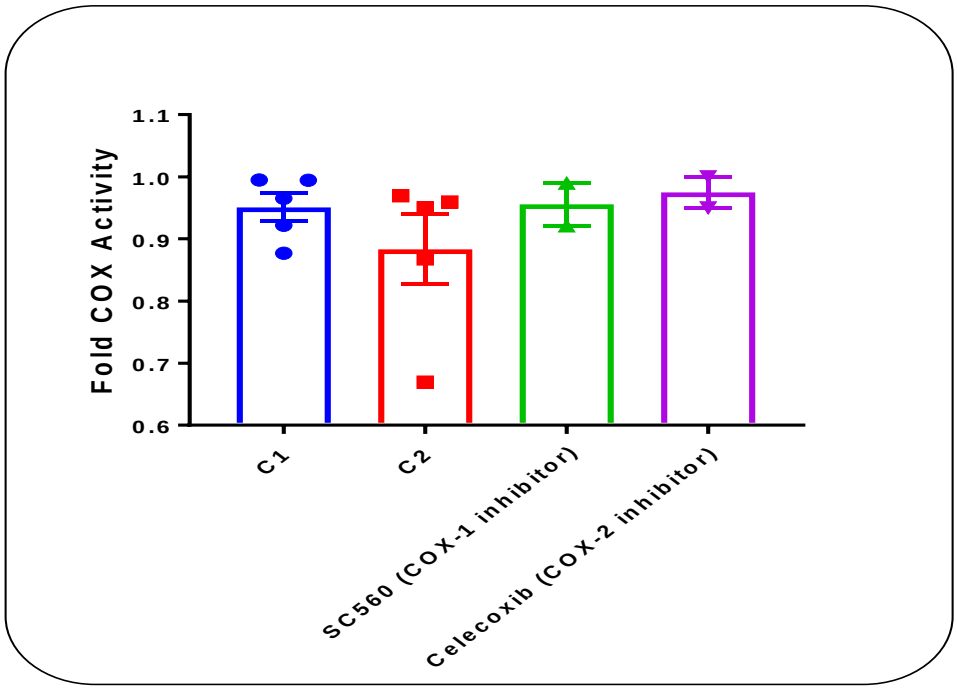

Figure 8: Measurement of COX activity of C1 and C2 compounds with Cyclooxygenase activity assay Kit.

3. ADME properties of compounds P1 and P2

The final synthesized compounds' physicochemical and ADME properties were investigated by the Swiss ADME server [18] to predict which of the synthesized ligands are susceptible to be given orally and to reveal the safe and possible drug candidate, to exclude the compounds that may fail in the next stages of the drug development because of the inappropriate ADME properties. [19] We assessed both synthesized compounds' pharmacokinetic properties, The results of all our synthesized compounds showed that TPSA values were less than 140, which were (54.77 and 67.32), for P1 and P2 respectively, and the bioavailability score for both ligands was 0.55, indicating that both reached the systemic circulation, as shown in the **Figures (9 and 10)**.

In our analysis, all synthesized ligands had high GI absorption, expecting them to be well absorbed from the intestine. [19] Regarding the toxicity of the synthesized compounds, the results of compound P2 are good with no alert, while P1 is only alert for aniline di-alkyl, as illustrated in **figures (9 to 11)**. The lipophilicity of both compounds is within the normal range.

The graphical output of all calculations was displayed by the BOILED-EGG figure by which two primary ADME parameters, passive absorption from the GI tract and BBB entry can be predicted, as shown in **figure 11**.

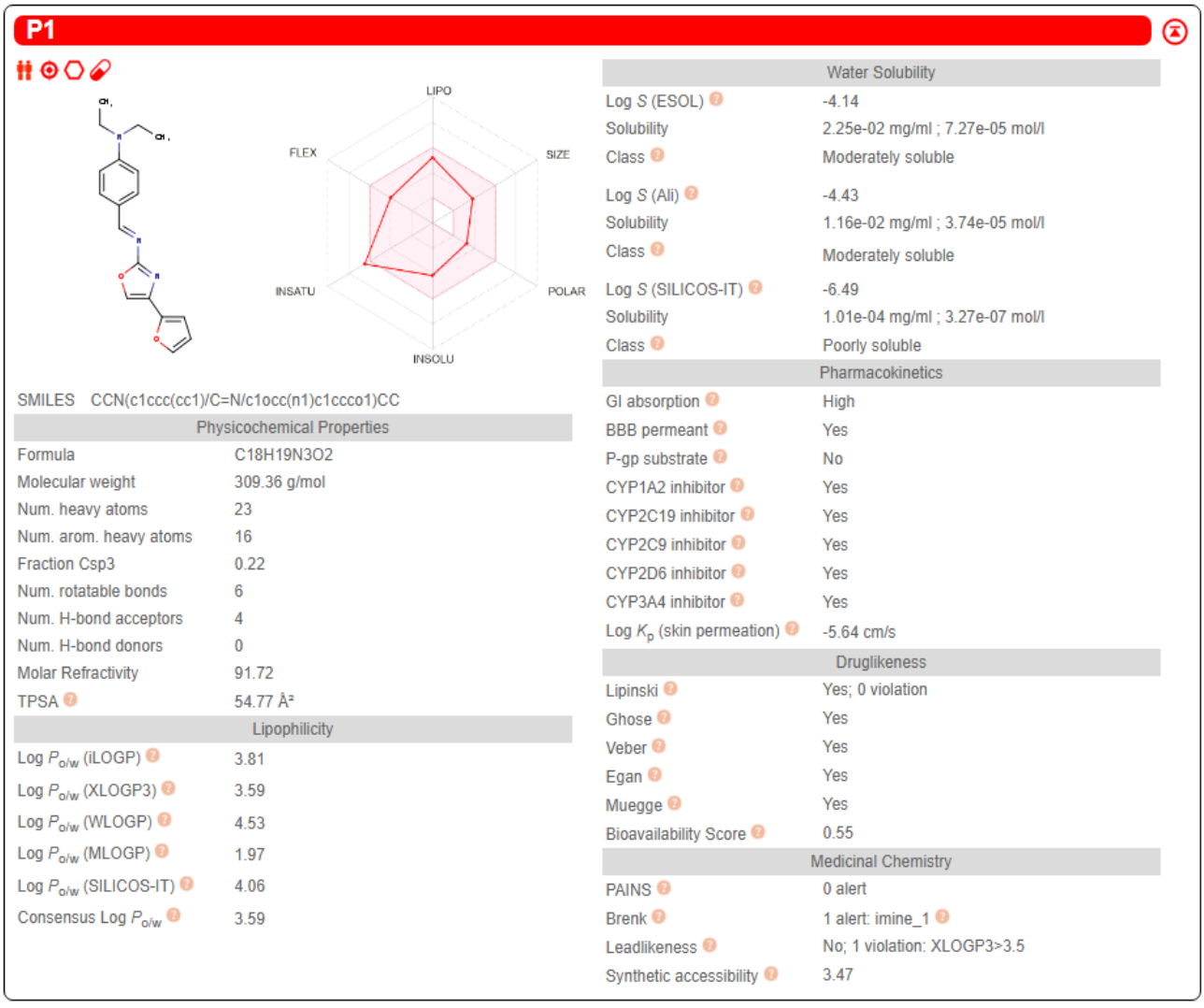

Figure 9: ADME study of Compound (P1).

P2

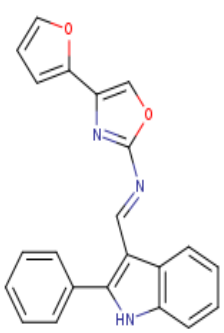

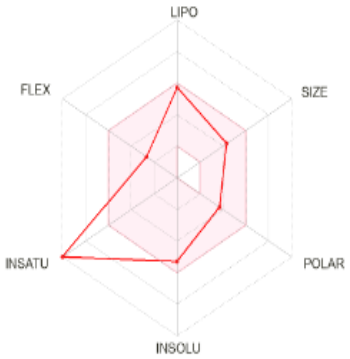

SMILES c1ccc(cc1)c1[nH]c2c(c1/C=N/c1occ(n1)c1ccco1)cccc2

Physicochemical Properties	
Formula	C22H15N3O2
Molecular weight	353.37 g/mol
Num. heavy atoms	27
Num. arom. heavy atoms	25
Fraction Csp3	0.00
Num. rotatable bonds	4
Num. H-bond acceptors	4
Num. H-bond donors	1
Molar Refractivity	105.19
TPSA	67.32 Å²

Lipophilicity	
Log $P_{o/w}$ (iLOGP)	3.35
Log $P_{o/w}$ (XLOGP3)	4.52
Log $P_{o/w}$ (WLOGP)	5.83
Log $P_{o/w}$ (MLOGP)	2.51
Log $P_{o/w}$ (SILICOS-IT)	5.74
Consensus Log $P_{o/w}$	4.39

Water Solubility	
Log *S* (ESOL)	-5.30
Solubility	1.77e-03 mg/ml ; 5.02e-06 mol/l
Class	Moderately soluble
Log *S* (Ali)	-5.66
Solubility	7.81e-04 mg/ml ; 2.21e-06 mol/l
Class	Moderately soluble
Log *S* (SILICOS-IT)	-8.94
Solubility	4.05e-07 mg/ml ; 1.15e-09 mol/l
Class	Poorly soluble

Pharmacokinetics	
GI absorption	High
BBB permeant	No
P-gp substrate	Yes
CYP1A2 inhibitor	Yes
CYP2C19 inhibitor	Yes
CYP2C9 inhibitor	No
CYP2D6 inhibitor	Yes
CYP3A4 inhibitor	No
Log K_p (skin permeation)	-5.25 cm/s

Druglikeness	
Lipinski	Yes; 0 violation
Ghose	No; 1 violation: WLOGP>5.6
Veber	Yes
Egan	Yes
Muegge	Yes
Bioavailability Score	0.55

Medicinal Chemistry	
PAINS	0 alert
Brenk	1 alert: imine_1
Leadlikeness	No; 2 violations: MW>350, XLOGP3>3.5
Synthetic accessibility	3.60

Figure 10: ADME study of Compound (P2).

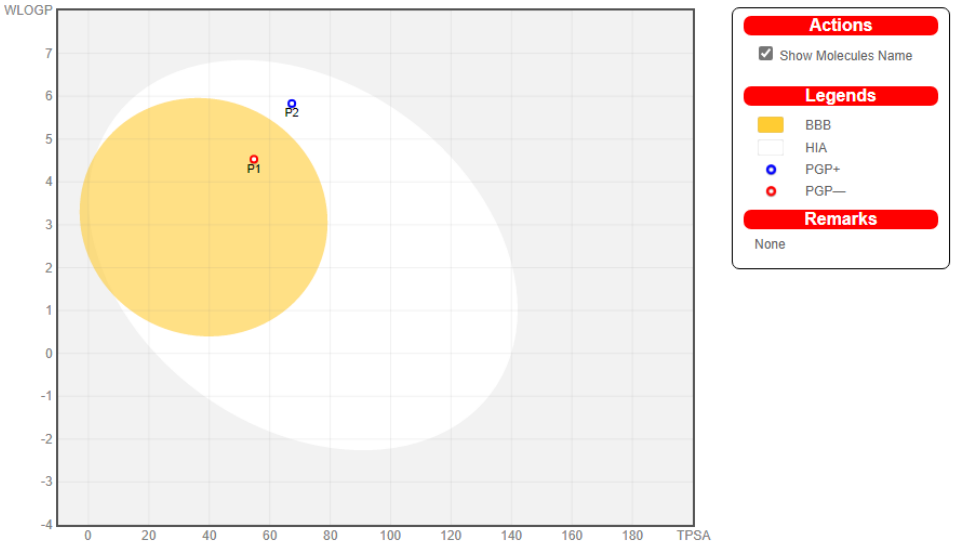

Figure 11: BOILED EGG – for final compounds.

Yellow ovule (yolk): a molecule that is expected to move through blood-brain barriers passively.

White ovule (white): The GIT is expected to absorb this molecule passively.

PGP+: Blue dots indicate that the molecules are effluxed from the CNS by the PGP.

PGP-: Red dots indicate that the molecules are not effluxed from the CNS by the PGP.[109]

Experimental Work

1. General

All reagents and anhydrous solvents were used as received from the commercial suppliers (Merck, Darmstadt, Germany, Sigma-Aldrich, Munich, Germany, BDH, Pool Dorset, England, and Fluka, Newport News, USA). 2-acetyl furan was purchased from Sigma-Aldrich (Shanghai, China). Melting points were determined by the capillary method using the electrothermal melting point apparatus (Stuart company). Thin layer chromatography (TLC) was run on Silicagel (60) F_{254} (Merck) to check the purity of the products as well as to monitor the progress of reactions. The identification of compounds was done using FT-IR spectra recorded by using a Shimadzu model (Kyoto, Japan) spectrophotometer on KBr disks, ^{1}H-NMR spectra was recorded in d_6-DMSO using Inova-Varian, Agilent 500MHz. **Scheme 1** defines the whole synthetic pathway.

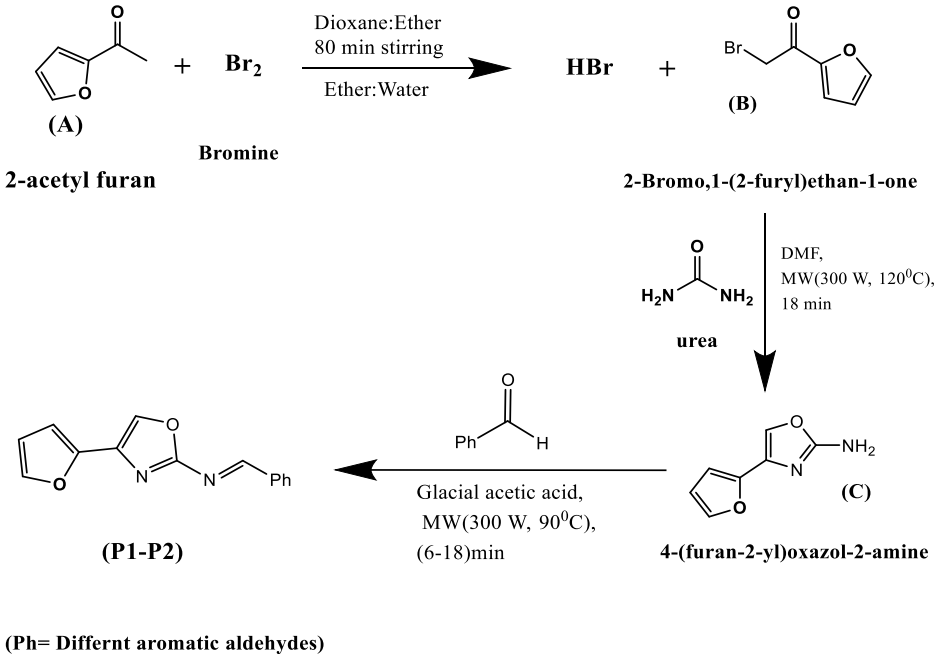

Scheme 1. Synthetic pathway of oxazole Schiff base derivatives.

2. Procedure for furan-2-carbonyl bromide synthesis

To a solution of (0.1 mol,11gm) 2-acetyl furan (**A**) in a mixture of 20 mL of dioxane and 50 mL of diethyl ether at (20-25)°C with vigorous stirring for (60 min.), (0.1 mol) of bromine was added dropwise. An eye-irritant fume was being produced during the stirring process and a brown-oily product start to take place. The mixture was stirred for a further 20 minutes and poured onto 60gm of iced water and 20 mL of diethyl ether. In the separatory funnel, the mixture has been extracted up to three times, washed with saturated sodium bicarbonate solution (8gm/100Ml water), and dried with magnesium sulfate anhydrous. Vacuum distillation was applied to remove excess ether and an oily-brown colored product was obtained (compound **B**)and preserved cold in a diethyl ether solvent (85% yield). [20] *2-Bromo-1-(furan-2-yl)ethan-1-one* boiling point 235°C. IR 3032 Aromatic (C-H), 1676 Carbonyl (C=O), 1566 cyclic alkene (C=C), 767 Aromatic stretching, and 644 strong bending of (C-Br).

3. Procedure for furan oxazole amine synthesis

After grinding (0.1 mol or 6 gm;10 equivalent) of urea and sequenced addition of the powder to an already (70°C) hot-stirred DMF solvent (10 mL) in a beaker, the hot dissolved urea in dry DMF solvent was added directly to a G30 vial containing (0.01 mol;1 equivalent) of 2-Bromo-1-(furan-2-yl)ethan-1-one (**B**), that's already being stirred. The reaction mixture was irradiated in a microwave reactor after setting the parameters as follows: temperature (120°C), time is 18 minutes, pressure 250 psi, and power is 300 W. After completion of the reaction, confirmed using TLC (95:5 dichloromethane/methanol), a red wine-like solution produced and water was added followed by extraction with ethyl acetate that is done up to three times. The organic layer was washed with brine (3gm/10 mL) and dried over magnesium sulfate anhydrous. After filtration, ethyl acetate was removed using vacuum distillation. [21 & 22] The oily red-wine-colored product was collected as compound **C** (56% yield). *5-(furan-2-yl)oxazol-2-amine* M.p. 139°C. IR 3500 Primary amine (NH2), 1668 (C=N), 1599 cyclic alkene (C=C), 1298-1084 bending of two bands (C-O), and 752 Aromatic stretching.

4. General procedure for oxazole Schiff base derivatives synthesis, compounds (P1 and P2)

(0.01mol) of compound (**C**) is to be added to (0.01mol) of one of the aldehydes (a and b) that have been already dissolved in (65 °C) hot-stirred 10 mL methanol (amount added gradually to ensure quick dissolution) with drops of glacial acetic acid added to the dissolved aldehyde solution and left to hot stir for 10 minutes. The reaction mixture was then transferred to a G30 vial and subjected to microwave irradiation while setting the parameters as follows: temperature (90 -120) °C, time is specific for each aldehyde, pressure 250 psi, and power is 300 W. At the end of this time, the reaction mixture was added to a beaker with cold, distilled water and crushed ice to stop the reaction. The yield products with colored powder are vacuum filtered using a Buchner funnel and recrystallized from ethanol. [23 & 24] **Table 1** shows the aldehydes used and the time required for irradiation. Moreover, **Table 2** defines the Structures and names of synthesized compounds.

(E)-N,N-diethyl-4-(((4-(furan-2-yl)oxazol-2-yl)imino)methyl)aniline (**P1**), dark brown oily liquid (85% yield). IR 2970 secondary amine (CH3), 1662 Schiff base (C=N), 1587 aromatic (C=C) bond, 1240-1152 (C-O) Stretching with two bands, and 814 Aromatic para di subistituted (790-840) cm−1. ^{1}HNMR 1.12 (t, 6H, CH3 of tertiary amine), 3.43 (q, 4H, CH2 of tertiary amine), 6.70 (d, 2H, of aromatic ring), 7.06 (t, 1H, of furan H), 7.60 (d, 2H, of aromatic ring), 7.64 (d, 1H, of furan H), 7.65 (s, 1H, oxazole H), 7.83 (d, 1H, of furan H), and 9.13 (s, 1H, CH of imine group) ppm.

(E)-N-(4-(furan-2-yl)oxazol-2-yl)-1-(2-phenyl-1H-indol-3-yl)methanimine (**P2**), Dark red crystals (87% yield). M.p. (210-215) °C. IR 3448 (N-H) secondary amine, 1650 (C=N) Stretching, 1577 Aromatic (C=C), 1373 oxazole (C-N), 1080-1168 (C-O) Stretching of two bands, 1016 (C-N) stretching of the imidazole, and 694-742 Aromatic mono substituted two bands. ^{1}HNMR 7.22 (t, 1H, Furan H), 7.24 (t, 1H, aromatic H of indole), 7.25 (t, 1H, aromatic H of indole), 7.48 (t, 1H, Aromatic H), 7.52 (t, 2H, Aromatic H), 7.59 (d, 1H, Furan H), 7.64 (t, 1H, Aromatic H of indole), 7.75 (s, 1H, Oxazole H), 7.84 (d, 2H, Aromatic H), 8.23 (d, 1H, Furan H), 8.27 (d, 1H, aromatic H of indole), 9.98 (s, 1H, imine group), and 12.38 (s, 1H, N-H group) ppm.

Table 1: Aldehydes with the time required for irradiation.

	Aldehyde	Aldehyde	Temperature applied	Time required for the reaction
a	4-Diethylaminobenzaldehyde	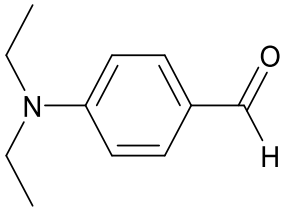	90°C	6 minutes
b	2-Phenylindole-3-carboxylic Acid	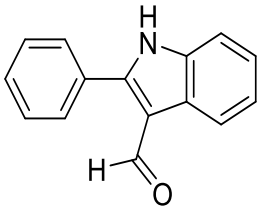	100°C	36 minutes

Table 2: Structures and names of synthesized compounds

Compound	Structure	IUPAC Name	SMILE Notation
2-Acetyl Furan (A)	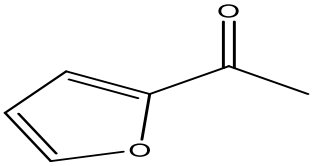	1-(furan-2-yl)ethan-1-one	O=C(C1=CC=CO1)C
B	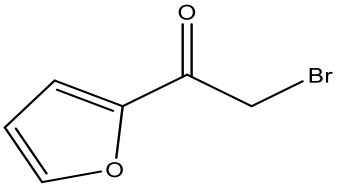	2-Bromo-1-(furan-2-yl)ethan-1-one	O=C(C1=CC=CO1)CBr
C	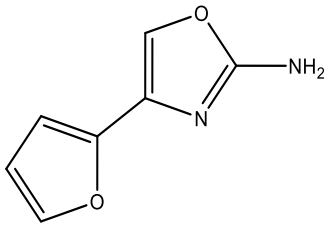	5-(furan-2-yl)oxazol-2-amine	NC1=NC(C2=CC=CO2)=CO1
P1	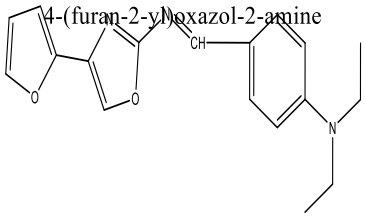	(E)-N,N-diethyl-4-(((4-(furan-2-yl)oxazol-2-yl)imino)methyl)aniline	CCN(C1=CC=C(/C=N/C2=NC(C3=CC=CO3)=CO2)C=C1)CC
P2	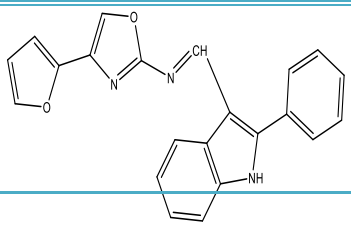	(E)-N-(4-(furan-2-yl)oxazol-2-yl)-1-(2-phenyl-1H-indol-3-yl)methanimine	C1(C2=COC(/N=C/C3=C(C4=CC=CC=C4)NC5=C3C=CC=C5)=N2)=CC=CO1

5. In vitro COX-1/COX-2 inhibition assay in RAW 264.7 cell line

The in vitro ability of the tested (P1 and P2) compounds to inhibit COX-1 and COX-2 isoenzymes were determined using a cyclooxygenase activity assay (Fluorometric) kit. Firstly, harvest 2×106 RAW 264.7 cells in a 75 cm2 flask at 24 h. After that, washed cells with 10 mL cold PBS (1X) and transferred cells to a 1.5 mL tube. Centrifuged at 500 x g for 3 minutes and discard the supernatant and resuspend the cell pellet in 0.2 – 0.5 mL of lysis buffer with a protease inhibitor cocktail. Then, incubated on ice for 5 minutes and centrifuged the cell lysate at 12,000 x g, 4°C for 3 minutes. 200 µl of cell lysate was added to every 12 well plates then added100µL from 1 – 5µM of P1 and P2 compounds, SC560 (COX-1 inhibitor as a positive control), and Celecoxib (COX-2 inhibitor as a positive control) to the inhibitor wells for the enzyme and 20 µL of vehicle (DMSO) were added to 100% initial activity and background wells. The plate was incubated for 10 min at 37 °C and the reaction was started by adding 580 µL of the reaction mixture (20µl COX Probe + 40µl COX Cofactor + 520µl COX assay buffer) into each well, then immediately injecting 100 µL of diluted cold arachidonic acid solution to all the reaction well. After the addition of the arachidonic acid, measured fluorescence at (Ex/Em = 535/587 nm).

REFERENCES

Schmid-Schonbein G W, Analysis of Inflammation. Annu. Rev. Biomed. Eng. 2006; 8: 93–151.

Nathan, C. Points of control in inflammation. Nature. 2002; 420: 846–852.

Medzhitov R. Origin and physiological roles of inflammation. Nature 2008; 454: 428–435.

Bhatelia K., Singh K., Singh R. TLRs: Linking inflammation and breast cancer, ELSEVIER. 2014; 26 (11), 2350-2357.

Gomes M., Teixeira A. L., Coelho A., Araújo A., and Medeiros R. The Role of Inflammation in Lung Cancer. Springer. 2014; pp 1–23.

Li S, Jiang M, Wang L, Yu S. Combined chemotherapy with cyclooxygenase-2 (COX-2) inhibitors in treating human cancers: Recent advancement. Biomedicine & Pharmacotherapy. 2020 Sep; 129: 110389.

Ballaz S., Mulshine J. L. The Potential Contributions of Chronic Inflammation to Lung Carcinogenesis. Clinical Lung Cancer. 2003; 5(1): 46-62.

Khudhair M. A., Mahdi M. F., Khan A. K., Abd Razik B. M. Molecular Modeling, Drug Design and Binding Evaluation of New Oxazole Derivatives as Cyclooxygenase Inhibitors. Egypt. J. Chem. 2021; 64 (9): 5101 – 5109.

Ahmadi M., Bekeschus S., Weltmann K. D., Woedtke T. V., and Wende K. Non-steroidal anti-inflammatory drugs: recent advances in the use of synthetic COX-2 inhibitors. RSC Med. Chem., 2022; 13, 471-496.

Linton MF, Fazio S. Cyclooxygenase products and atherosclerosis. Drug Discov Today Ther Strateg. 2008; 5(1): 25-36.

Rouzer CA, Marnett LJ. Cyclooxygenases: structural and functional insights. J Lipid Res. 2009; 50 Suppl(Suppl): S29-S34.

Singh N., Bhati K. S., Kumar A. Thiazolyl/oxazolyl formazanyl indoles as potent anti-inflammatory agents. Eur. J. Med. Chem. 2008; 43(11): 2597-2609.

Lin Y., Ahmed W., He M., Xiang X., Tang R. Cui Z.-N. Synthesis and bioactivity of phenyl substituted furan and oxazole carboxylic acid derivatives as potential PDE4 inhibitors. J EJMCH. 2020; 112795.

Kumar S., Saroha B., Kumar G., Lathwal E., Kumar S., Parshad B., Kumari M., Kumar N., Mphahlele-Makgwane M.M., Makgwane P.R. Recent Developments in Nanocatalyzed Green Synthetic Protocols of Biologically Potent Diverse O-Heterocycles—A Review. Catalysts. 2022; 12(6): 657.

Rymbai E. M., Chakraborty A., Choudhury R., Verma N., De B. Review on Chemistry and Therapeutic Activity of the Derivatives of Furan and Oxazole: The Oxygen Containing Heterocycles. Der Pharma Chemica. 2019; 11(1): 20-41.

Chaudhary KK, Mishra N. A Review on Molecular Docking: Novel Tool for Drug Discovery. JSM Chem. 2016; 4(3): 1029.

Liebeschuetz, J.W., Cole, J.C. & Korb, O. Pose prediction and virtual screening performance of GOLD scoring functions in a standardized test. J Comput Aided Mol Des. 2012; 26: 737–748.

Daina, A. et al. SwissADME: a free web tool to evaluate pharmacokinetics, drug-likeness and medicinal chemistry friendliness of small molecules. Sci. Rep. 2017: 7: 42717.

Adnan A. M. A., Mahdi M. F., Khan A. K. Design, Synthesis, and Acute Anti-inflammatory Assessment of New 2-methyl Benzoimidazole Derivatives Having 4-Thiazolidinone Nucleus. Al Mustansiriyah J Pharm Sci. 2019; 19(4): 151–60.

Saldabol N., Popelis Yu., Shatz V., and Slavinskaya V. Bromination of 2-acetyl-5-methylfuran. Chemistry of Heterocyclic Compounds. 1999; 35 (2).

Dubac J., Gaset A., and Maraval M. An Easy Synthesis of 2-Haloacetylfurans and Thiophenes. Synth Commun. 1991; 21(1): 11-16.

Güven Ö. Ö., Erdo T., Göker H., Yıldız S. Synthesis and Antimicrobial Activity of Some Novel Furyl and Benzimidazole Substituted Benzyl Ethers. J. Heterocyclic Chem. 2007; 44, 731.

McMurry J.Organic Chemistry. (7th Ed.).2008; pp.751.

Celik H. Microwave-assisted synthesis and antibacterial activities of some N-Benzylideneaniline halogen derivatives. Fresenius Environ. Bull. 2019; 28 (7): 5367-5381.